Title
Intestinal serotonin and fluoxetine exposure modulate bacterial colonization in the gut

Journal
Nature Microbiology, 4(12)

ISSN
2058-5276

Authors
Fung, Thomas C
Vuong, Helen E
Luna, Cristopher DG
et al.

Publication Date
2019-12-01

DOI
10.1038/s41564-019-0540-4

Peer reviewed

HHS Public Access

Author manuscript

Nat Microbiol. Author manuscript; available in PMC 2020 March 02.

Published in final edited form as:

Nat Microbiol. 2019 December ; 4(12): 2064–2073. doi:10.1038/s41564-019-0540-4.

Intestinal serotonin and fluoxetine exposure modulate bacterial colonization in the gut

Thomas C. Fung[1,*], **Helen E. Vuong**[1], **Christopher D.G. Luna**[1], **Geoffrey N. Pronovost**[1], **Antoniya A. Aleksandrova**[2], **Noah G. Riley**[2], **Anastasia Vavilina**[1], **Julianne McGinn**[1], **Tomiko Rendon**[1], **Lucy R. Forrest**[2], **Elaine Y. Hsiao**[1,*]

[1]Department of Integrative Biology & Physiology, University of California Los Angeles, Los Angeles, CA 90095, USA

[2]Computational Structural Biology Unit, National Institute of Neurological Disorders and Stroke, National Institutes of Health, Bethesda, MD 20892, USA

Abstract

The gut microbiota regulates levels of serotonin (5-hydroxytryptamine, 5-HT) in the intestinal epithelium and lumen[1–5]. However, whether 5-HT plays a functional role in bacteria from the gut microbiota remains unknown. We demonstrate that elevating levels of intestinal lumenal 5-HT by oral supplementation or by genetic deficiency in the host 5-HT transporter (SERT) increases the relative abundance of spore-forming members of the gut microbiota, which were previously reported to promote host 5-HT biosynthesis. Within this microbial community, we identify *Turicibacter sanguinis* as a gut bacterium that expresses a neurotransmitter sodium symporter (NSS)-related protein with sequence and structural homology to mammalian SERT. *T. sanguinis* imports 5-HT through a mechanism that is inhibited by the selective 5-HT reuptake inhibitor, fluoxetine. 5-HT reduces expression of sporulation factors and membrane transporters in *T. sanguinis*, which is reversed by fluoxetine exposure. Treating *T. sanguinis* with 5-HT or fluoxetine modulates its competitive colonization in the gastrointestinal tract of antibiotic-treated mice. In addition, fluoxetine reduces the membership of *T. sanguinis* in the gut microbiota of conventionally-colonized mice. Host association with *T. sanguinis* alters intestinal expression of multiple gene pathways, including those important for lipid and steroid metabolism, with corresponding reductions in host systemic triglyceride levels and inguinal adipocyte size. Altogether, these findings support the notion that select bacteria indigenous to the gut microbiota signal bidirectionally with the host serotonergic system to promote their fitness in the intestine.

*Correspondence to: tcfung@ucla.edu and ehsiao@g.ucla.edu.

Author Contributions: T.C.F. performed bacteriology and sequencing experiments, C.D.G.-L. and A. V. assisted with bacteriology experiments, T.C.F., H.E.V. and G.N.P. performed mouse experiments, A.A.A., N.G.R. and L.R.F. performed structural modelling, J.M. and T.R. generated gnotobiotic mice, L.R.F. and E.Y.H. contributed to data analysis, T.C.F., L.R.F. and E.Y.H. supervised the study.

Competing Interests: The authors declare no competing interests. Findings regarding the host effect of *T. sanguinis* reported in the manuscript are the subject of provisional patent application US 62/815,760, owned by UCLA.

The gut microbiota regulates several host biochemicals with known neuromodulatory properties, including endocannabinoids, neuropeptides and biogenic amines[6]. Of these, the hormone and neurotransmitter serotonin (5-hydroxytryptamine, 5-HT) is expressed highly in the gastrointestinal tract, synthesized by enterochromaffin cells (ECs) to levels that account for over 90% of the body's 5-HT content[7]. Approximately 50% of gut-derived 5-HT is regulated by the gut microbiota, particularly spore-forming bacteria dominated by the families *Clostridiaceae* and *Turicibacteraceae*, with downstream consequences on host intestinal motility, hemostasis and ossification[1–5]. However, whether microbial regulation of host 5-HT occurs as a side effect of bacterial metabolism, or whether there is a functional role for microbial regulation of host 5-HT on bacterial physiology remains unclear. Interestingly, while the majority of gut 5-HT is secreted basolaterally by ECs into surrounding intestinal tissues, some EC-contained 5-HT is secreted apically into the intestinal lumen[3,5,8], suggesting that gut microbes are exposed to host-derived 5- HT. Indeed, microbial influences on host ECs regulate 5-HT levels not only in intestinal tissue and blood1–4, but also in the intestinal lumen and feces[3,5,8], raising the question of whether there are direct effects of host-derived 5-HT on gut bacteria.

To determine whether the microbiota responds to intestinal 5-HT, we used three approaches to elevate lumenal 5-HT levels and measure their effects on microbiota composition. As a first proof- of-concept, we supplemented specific pathogen-free (SPF) mice orally with 5-HT to increase fecal 5-HT levels relative to vehicle-treated controls (Fig. 1a). 5-HT substantially enriched species of *Clostridia* from a combined relative abundance of 10.3 ± 1.9% (mean ± S.E.M.) in SPF mice to 86.2 ± 5.8% in 5-HT-supplemented mice (Fig. 1b–d and Supplementary Table 1). This is consistent with prior research demonstrating that spore-forming bacteria dominated by *Clostridiaceae* and *Turicibacteraceae* sufficiently promote gut 5-HT3. To determine whether physiological increases in host-derived 5-HT similarly alter the gut microbiota, we utilized serotonin transporter (SERT)- deficient mice which exhibit modest elevations in 5-HT along the intestine[9]. SERT deficiency increased fecal 5-HT by 1.7-fold in $SERT^{+/-}$ mice (Fig. 1e) and enriched *Clostridiaceae* and *Turicibacter* from a combined 0.9 ± 0.3% in wildtype mice to 13.7 ± 5.5% (Fig. 1f–i and Supplementary Table 2). Notably, these changes were more pronounced in $SERT^{+/-}$ mice, which lack confounding abnormalities in gastrointestinal motility and behavior, as compared to $SERT^{-/-}$ mice[10]. To further determine whether genetic predisposition to elevated intestinal 5-HT shapes the gut microbiota, we re-derived the SERT mouse line as germ-free (GF) and inoculated $SERT^{+/-}$ GF mice and wildtype GF controls with the same SPF fecal microbiota (Supplementary Data Fig. 1a). At 1 day after inoculation, we observed no overt taxonomic differences; however, at 35 days, $SERT^{+/-}$ mice exhibited significantly increased levels of *Clostridia*, including *Clostridiales*, *Lachnospiraceae* and *Ruminococcaceae* (Supplementary Data Fig. 1b–e and Supplementary Table 3). Overall, these findings reveal that increasing intestinal 5-HT enriches for spore-forming bacteria. This supports the notion that induction of host 5-HT by spore-forming bacteria[3] promotes their own community membership in the gut microbiota.

The ability of the microbiota to respond to elevations in host 5-HT suggests that select gut bacteria may encode elements for sensing 5-HT. To evaluate this possibility, we mined bacterial genomes for orthologs of mammalian (human or mouse) SERT. We identified a top candidate with 34% amino acid sequence identity (Supplementary Data Fig. 2a–b) and

predicted structural homology to mammalian SERT (Fig. 2j), which is encoded by all four sequenced strains of the filamentous gut bacterium *Turicibacter sanguinis* and *Turicibacter* spp. (Supplementary Table 4). The gene is annotated for *T. sanguinis* HGF1 as a "putative sodium-dependent 5-HT transporter," and has greater homology to SERT than to LeuT, a promiscuous bacterial amino acid transporter used to model eukaryotic neurotransmitter sodium symporter (NSS) proteins (Supplementary Data Fig. 2a). Interestingly, *Turicibacter* was enriched particularly in $SERT^{+/-}$ mice, which exhibited increased lumenal bioavailability of 5-HT (Fig. 1g–h). Moreover, *Turicibacter* was the most abundant member of the spore-forming bacterial consortium previously shown to induce host 5- HT biosynthesis (Fig. 2a–c, Supplementary Table 5 and [3]), and correlated with intestinal 5-HT levels (Fig. 2d–e).

We generated a model of the *Turicibacter* protein based on available structures of human SERT. Given the level of amino acid sequence identity (>30%) between the template and the target sequence, the expected accuracy of this model is 0.7–2.0 Å for the backbone of the transmembrane regions[11]. Indeed, the model scores very highly, consistent with the *Turicibacter* protein being globally similar to hSERT (Supplementary Data Fig. 3a–e). Residues contributing to the 5-HT and selective 5-HT reuptake inhibitor (SSRI) binding sites in mammalian SERT[12] are strongly conserved (~50% identical and ~70% similar), and the residues required to bind a Na+ ion at the so-called Na2 site are identical. However, there were differences in key residues that mediate Cl^--dependence (N368, replaced by D262) and neutralization of charged amines (D98, replaced by G22) in mammalian SERT[13,14]. The latter in particular raises the question of whether the bacterial ortholog is capable of transporting 5-HT. However, the concurrent substitution of N368 in hSERT by an acidic side chain (D262) just 7 Å away raises the possibility that D262 can play a similar role to D98, allowing for a slightly altered arrangement for 5-HT or inhibitors in a similar binding region.

To determine whether *Turicibacter* is able to detect, import or metabolize 5-HT, we examined the ability of *T. sanguinis* MOL361 to i) consume 5-HT in culture, ii) import 4-(4-(dimethylamino)phenyl)-1-methylpyridinium (APP+), a molecular substrate for SERT[15], iii) uptake radiolabeled 5-HT, and iv) respond transcriptionally to 5-HT. Culturing *T. sanguinis* in nutrient-rich broth decreased 5-HT levels in the media over time (Fig. 2f). This was prevented by supplementation with the SSRI fluoxetine, a reversible inhibitor of SERT (Fig. 2f), which exhibited cytostatic effects over long-term culture (Supplementary Data Fig. 4) but not short- term exposure (Fig. 3h, Supplementary Discussion). Exposing *T. sanguinis* to APP+ resulted in import, which was partially decreased by bacterial pre-treatment with unlabeled 5-HT or fluoxetine (Fig. 2g–h). There was also a modest, but not statistically significant, effect of norepinephrine, but not dopamine, on decreasing APP+ uptake in the assay (Supplementary Data Fig. 5a). Moreover, *T. sanguinis* imported tritiated 5-HT ([3H]5-HT), which was inhibited by fluoxetine (Fig. 2i). Notably, fluoxetine had no effect on bacterial uptake of norepinephrine (Supplementary Data Fig. 5b), suggesting some selectivity to inhibition of 5-HT import.

Inhibition of 5-HT uptake was not observed by treatment with reserpine or tetrabenazine, inhibitors of mammalian vesicular monoamine transporter (VMAT) (Supplementary Data Fig. 5c), suggesting that import of 5-HT by *T. sanguinis* is mediated by an NSS-like protein

such as the SERT ortholog (Fig. 2j) rather than a protein in the major facilitator superfamily (MFS), such as VMAT.

To gain insight into whether 5-HT uptake by *T. sanguinis* is mediated by the candidate protein, we cloned the gene from *T. sanguinis* MOL361 ("CUW_0748", as annotated for *T. sanguinis* PC909) into the intestinal bacterium *Bacteroides thetaiotaomicron*, which shows no evidence of endogenous APP+ import (Supplementary Data Fig. 6a). Heterologous expression of CUW_0748 in *B. thetaiotaomicron* (Supplementary Data Fig. 6b–c) conferred uptake of APP+ and 1 uM [3H]5- HT, which was inhibited by unlabeled 5-HT (Fig. 2k–l). CUW_0748 in *B. thetaiotaomicron* exhibited time-dependent saturation of [3H]5-HT import (Supplementary Data Fig. 6d), requiring longer durations than those reported for SERT expressed in mammalian systems[16,17]. Notably, however, CUW_0748 in *B. thetaiotaomicron* failed to show dose-dependent saturation of [3H]5- HT import; biological variation increased substantially with concentrations of [3H]5-HT higher than physiological range (>100 uM), which may be due to stress to *B. thetaiotaomicron*. This indicates that additional studies are needed to validate active transporter-mediated 5-HT import. Notably, there was no effect of CUW_0748 expression on uptake of tryptophan (Supplementary Data Fig. 6f), suggesting that it does not function as a tryptophan transporter or broadly disrupt bacterial membrane integrity. These findings suggest that CUW_0748 contributes to 5-HT uptake in *T. sanguinis*, but also leave open the possibility that additional mechanisms for 5-HT import exist. Moreover, it is unclear whether the SERT ortholog, or any unknown 5-HT response elements in *Turicibacter*, are specific to 5-HT as opposed to other biogenic amines, indole derivatives or amino acids. While more research is required to detail the structural and biochemical properties of CUW_0748, these findings demonstrate that *T. sanguinis* imports 5-HT at physiological levels, which is inhibited by fluoxetine, suggesting that transport through an NSS-like protein mediates bacterial 5-HT uptake.

To identify effects of 5-HT and fluoxetine on bacterial physiology, we profiled transcriptomes of *T. sanguinis* after acute exposure to vehicle, 5-HT, fluoxetine or 5-HT with fluoxetine. 5-HT significantly altered bacterial expression of 71 genes (Fig. 3a–b), suggesting that *T. sanguinis* responds functionally to 5-HT. Co-treatment of 5-HT with fluoxetine significantly altered 51 of the 71 genes that were differentially expressed in response to 5-HT alone, with additional changes in 344 genes, revealing substantial effects of fluoxetine on bacterial gene expression (Fig. 3a–b and Supplementary Table 6). In particular, 5-HT downregulated expression of genes that clustered into pathways for cell differentiation, morphogenesis and sporulation (Fig. 3c) and encoded proteins related to efflux transporters, ABC transporters and sporulation (Fig. 3d). Compared to 5- HT-treated controls, fluoxetine upregulated expression of genes encoding proteins relevant to efflux transporters, ABC transporters and sporulation (Fig. 3e), as well as energy metabolism, metal homeostasis and stress response, suggesting that fluoxetine prevents and/or reverses a subset of 5-HT-mediated changes in *T. sanguinis* gene expression. Consistent with fluoxetine-associated increases in expression of sporulation-related genes, imaging of *T. sanguinis* exposed to 5-HT with fluoxetine revealed punctate staining of the membrane dye FM 4–64 (Fig. 3f, g), a phenotype observed during spore formation[18]. Notably, fluoxetine treatment in the absence of 5-HT yielded little change in *T. sanguinis* gene expression (Supplementary Tables 6 and 7), indicating that 5- HT is required for fluoxetine-induced

alterations in gene expression. In addition, *T. sanguinis* survival was not affected by acute treatment with 5-HT and/or fluoxetine (Fig. 3h), suggesting that gene expression changes were not due to altered bacterial viability. Overall, these data demonstrate that 5-HT directly alters *T. sanguinis* physiology to reduce the expression of genes related to sporulation and membrane transport, which is abrogated by fluoxetine.

Sporulation is an important determinant of microbial colonization and transmission[19]. Given that 5-HT and fluoxetine regulate the expression of sporulation-related genes in *T. sanguinis*, we tested whether 5-HT and fluoxetine modulate *T. sanguinis* fitness in the intestine. *T. sanguinis* pre-treated with vehicle, 5-HT or 5-HT with fluoxetine was orally-gavaged into antibiotic-treated SPF mice supplemented with the same chemical treatments in drinking water. Both vehicle and 5-HT treatment resulted in detectable *T. sanguinis* colonization (Fig. 3i–j). However, treatment with 5-HT and fluoxetine significantly reduced *T. sanguinis* levels in the small intestine (Fig. 3i– j, Supplementary Discussion) and colon (Supplementary Data Fig. 7a–b), suggesting that fluoxetine-mediated inhibition of 5-HT uptake impairs *T. sanguinis* colonization. Reductions in *T. sanguinis* were similarly seen without additional chemical supplementation in the drinking water, where pre-treatment of *T. sanguinis* with 5-HT alone promoted its competitive colonization in antibiotic-treated mice (Supplementary Data Fig. 8a–d). In contrast, this effect was not seen with host supplementation alone (Supplementary Data Fig. 9a–b), suggesting that 5- HT and fluoxetine act directly on *T. sanguinis* to modulate intestinal colonization. Moreover, there was no effect of 5-HT and fluoxetine on *T. sanguinis* in monocolonized mice (Supplementary Data Fig. 10a–b) suggesting that 5-HT and fluoxetine do not affect the stability of *T. sanguinis* that has already colonized the intestine. In addition, there was no effect of 5-HT and fluoxetine on bacterial colonization of GF mice (Supplementary Data Fig. 11a–b), suggesting that 5-HT sensing by *T. sanguinis* is important for its competitive colonization within complex microbial communities and that fluoxetine is not broadly antimicrobial to *T. sanguinis* under these conditions. Consistent with this, SPF mice gavaged with fluoxetine exhibited decreased *Turicibacter* (Fig. 3k–m) and *Clostridiaceae*, with no significant differences in bacterial alpha diversity (Supplementary Data Fig. 12a–c). Collectively, these results suggest that inhibiting bacterial uptake of 5-HT and altering bacterial gene expression by fluoxetine limits the ability of *Turicibacter* to competitively colonize the intestine.

Changes in *Turicibacter* levels have been correlated with particular disease states[20]; however, causal effects of *Turicibacter* on the host remain unknown. To determine how *Turicibacter* colonization impacts host physiology, we first examined intestinal transcriptomes from *T. sanguinis* monocolonized mice, relative to GF and SPF controls. *T. sanguinis* differentially regulated 89 genes in the small intestine (Fig. 4a and Supplementary Table 8) and 87 genes in the colon (Supplementary Data Fig. 13a and Supplementary Table 9), which were enriched in pathways for steroid and lipid metabolism (e.g. *Hmgcs1, Insig1, Fift1, Msmo1, Hmgcr, Npc1l1*) (Fig. 4b–c and Supplementary Data Fig. 13b–c). This is likely not due to bacterial colonization in general, as there was little overlap between the effects of *T. sanguinis* versus SPF colonization on intestinal gene expression (Fig. 4a–b, Supplementary Data Fig. 13a–b and 14a–b). Moreover, *T. sanguinis*-induced transcriptomic changes were distinct from those reported in mice monocolonized with other species of gut bacteria[21]. In addition to altering intestinal expression of genes related to lipid metabolism,

T. sanguinis also reduced host serum triglyceride levels (Fig. 4d). Consistent with this, fluoxetine-induced decreases in *T. sanguinis* were associated with increased serum triglyceride levels compared to mice colonized with vehicle-treated *T. sanguinis* (Fig. 4e). There was no effect of *T. sanguinis* on total serum cholesterol, free fatty acid, low-density lipoprotein or high-density lipoprotein levels (Supplementary Data Fig. 15). To determine whether *T. sanguinis* modulates concentrations of specific lipid species, we profiled sera for 1100 lipids spanning cholesterol esters, ceramides, diacylglycerides, free fatty acids, hexosyl ceramides, lysophosphatidylcholines, lysophosphatidylethanolamines, phosphatidylcholines, sphingomyelins and triacylglycerides (Fig. 4f–h, Supplementary Data Fig. 16 and Supplementary Table 10). Principal components analysis yielded clustering of lipidomic profiles from *T. sanguinis*- monocolonized mice distinctly from SPF and GF controls (Supplementary Data Fig. 16a and Fig. 4f). 184 lipids were significantly altered by *T. sanguinis* (Supplementary Data Fig. 16b and Supplementary Table 10), including several triacylglycerides (Fig. 4g and Supplementary Data Fig. 16c). In particular, *T. sanguinis* reduced levels of long-chain triglycerides containing 18:1 and 20:1 fatty acids such as oleate and gadoleate, while increasing levels of long-chain triglycerides containing 20:4 and 20:5 polyunsaturated fatty acids such as arachidonate and eicosapentaenoate (Fig. 4h). The reductions in monoenoic triacylglycerides were consistent with transcriptomic results wherein *T. sanguinis* downregulated expression of stearoyl-coenzyme A desaturase 2 (*Scd2*) (Fig. 4c), a rate-limiting enzyme for oleate synthesis[22]. Consistent with reductions in triglyceride levels (Fig. 4d, e), *T. sanguinis*-colonized mice exhibited small multilocular adipocytes in inguinal white adipose tissue (Fig. 4i, Supplementary Data Fig. 17) and reduced mass of inguinal white adipose tissue in female, but not male, mice (Supplementary Data Fig. 18), suggesting that *T. sanguinis* regulates fat mass in a sex-specific manner. These results reveal that *T. sanguinis* modulates host lipid metabolism, and further suggest that regulation of *T. sanguinis* colonization by 5-HT and fluoxetine could have downstream consequences on host physiology (Supplementary Data Fig. 19).

Considerable progress has been made in understanding host-microbial interactions that control intestinal colonization of select microbial species such as *Bacteroides*[23] but little is known about the molecular determinants of microbial colonization and community membership for other groups of bacteria, including those belonging to the dominant phylum *Firmicutes*. In addition, previous studies on bacterial responses to norepinephrine fueled the concept of “microbial endocrinology”[24], but whether host-microbial interactions occur via other canonical neurotransmitters remains poorly understood. Here we identify a role for host-derived 5-HT and fluoxetine treatment in regulating the gut microbiota, including intestinal colonization of the gut bacterium, *T. sanguinis*. Based on our findings, we propose that particular bacteria indigenous to the gut microbiota, including *Turicibacter*, have co-evolved to induce host 5-HT[1,3,5,8] and further sense host-derived 5-HT in order to promote their competitive colonization in the intestine. We hypothesize that additional members of the gut microbiota, including particular *Clostridia*, may respond to 5-HT directly through as-yet uncharacterized 5-HT response elements or indirectly through other bacteria, such as *Turicibacter*. Findings from our study support the notion that bidirectional host-microbial signaling via the serotonergic system shapes bacterial communities within the gastrointestinal tract. Notably, a recent human study of >2700 twins concluded that SSRI use

is associated particularly with reduced *Turicibacteraceae* in humans, which is consistent with findings from our *in silico*, *in vitro* and *in vivo* animal experiments[25]. These findings, along with increasing associations of *Turicibacter* spp. with altered immune and metabolic conditions[26–28], raise the question of whether *Turicibacter* impacts host health and disease. Supporting this, we find that monocolonization with *T. sanguinis* alters intestinal lipid metabolism, systemic triglyceride profiles and white adipose tissue physiology in mice, which could be relevant to reported links between SSRI use and symptoms of metabolic syndrome[29,30]. Future studies are needed to investigate the cellular mechanisms by which 5-HT and fluoxetine regulate *T. sanguinis* colonization in the gut and whether fluoxetine-induced changes in the gut microbiota mediate any effects of the SSRI on host intestinal function, neurophysiology and behavior.

Methods

Mice

C57Bl/6 and SERT$^{-/-}$ mice were purchased from Jackson Laboratories, reared as SPF or C-section rederived as GF and bred in flexible film isolators at the UCLA Center for Health Sciences barrier facility. Breeding animals were fed “breeder” chow (Lab Diets 5K52). Experimental animals were fed standard chow (Lab Diets 5010). Colonization status was monitored weekly by aerobic and anaerobic bacterial cfu plating and by 16S rDNA qPCR from fecal DNA extracted and amplified using the MoBio PowerSoil kit, SYBR green master mix (ThermoFisher) and QuantStudio 5 thermocycler (ThermoFisher). 6–12 week old mice were randomly assigned to experimental groups, which included age- and sex-matched cohorts of males and females. Sample sizes for animal experiments were determined based on prior experience with the experimental paradigm, existing literature utilizing the experimental paradigm, or by power calculation. Samples derived from animals were blinded to the experimenter for imaging- and sequencing-based analyses. All experiments were performed in accordance with the NIH Guide for the Care and Use of Laboratory Animals using protocols approved by the Institutional Animal Care and Use Committee at UCLA.

5-HT supplementation in mice for microbiota profiling

Water was supplemented with 5-HT (Sigma Aldrich) at 1.5 mg/ml based on calculations from [31] and provided *ad libitum* to mice for 2 weeks. Amount of water consumed and mouse weight were measured on days 3, 7, 10 and 14 of treatment. Mice were sacrificed one day after treatment for 5- HT assays and fecal 16S rDNA profiling was conducted as described below.

5-HT measurements

Blood samples were collected by cardiac puncture and spun through SST vacutainers (Becton Dickinson) for serum separation. The entire length of the colon or 1 cm regions of the distal, medial and proximal small intestine was washed in PBS to remove luminal contents, and sonicated on ice in 10 s intervals at 20 mV in ELISA standard buffer supplemented with ascorbic acid (Eagle Biosciences). Fecal pellets and intestinal contents were weighed and homogenized at 50 mg/ml in ELISA standard buffer supplemented with

ascorbic acid. Serotonin levels were detected by ELISA according to the manufacturer's instructions (Eagle Biosciences). Readings from tissue samples were normalized to total protein content as detected by BCA assay or the 660nm Protein Assay (Thermo Pierce).

16S rDNA sequencing

Bacterial genomic DNA was extracted from mouse fecal samples using the MoBio PowerSoil Kit. The library was generated according to methods adapted from [32]. The V4 regions of the 16S rDNA gene were PCR amplified using individually barcoded universal primers and 30 ng of the extracted genomic DNA. The PCR reaction was set up in triplicate, and the PCR product was purified using the Qiaquick PCR purification kit (Qiagen). 250 ng of purified PCR product from each sample were pooled and sequenced by Laragen, Inc. using the Illumina MiSeq platform and 2 × 250bp reagent kit for paired-end sequencing. Operational taxonomic units (OTUs) were chosen by open reference OTU picking based on 97% sequence similarity to the Greengenes 13_5 database. Taxonomy assignment and rarefaction were performed using QIIME1.8.0[33]. Metagenomes were inferred from closed reference OTU tables using PICRUSt[34].

Sequence alignment and structural modeling

The Joint Genome Institute Integrated Microbial Genomes and Microbiomes and NCBI microbial genomes databases were searched for proteins with sequence similarity to human SERT. Phylogenetic trees were generated for the 15 bacterial candidates with highest alignment scores using MAFFT[35] and Phylo.io[36]. Primer sets were generated against the SERT homolog ZP_06621923.1 from *T. sanguinis* PC909 and used to sequence the homologous gene encoding CUW_0748 in *T. sanguinis* MOL361. Protein structural models were created in Phyre2[37] and with MODELLER 9v15[38], based on the highest-resolution available structure of human SERT, namely protein data bank, PDB[39] entry 5i6x chain A, an outward-open conformation bound to paroxetine at 3.14 Å resolution. After initially aligning their sequences using AlignMe v1.1 in PST mode[40], and inspection of the Ramachandran plot of the initial model, the alignment was refined at positions with strained backbone dihedral angles (see Supplementary Data Fig. 3a for final alignment), and the model was rebuilt. Based on analysis of the binding site conservation in the initial model, a Na+ ion was included at the Na2 site, using the position observed in a related hSERT template structure (PDB entry 5i71 chain A). 500 models were built using different seeds, and a single model was selected, specifically that with the highest ProQM[41] score and fewest Ramachandran outliers, according to PROCHECK[42]. To remove local clashes and optimize geometry, this model was energy-minimized using with the CHARMM36 force field[43] with NAMD v2.9[44], while constraining the backbone atoms and ion at Na2. Further quality assessment was carried out using MolProbity[45], and ConSurf[46] (Supplementary Data Fig. 3b, 3e). Structural models were visualized in Chimera[47] and PyMol v1.7 [Schrödinger, LLC]. Residues involved in 5-HT, Cl^- and Na+ binding in mammalian SERT were assessed based on existing literature[13,14,48]. The model is provided in the supplementary materials (Database S1).

Bacterial isolation and cultivation

Turicibacter sanguinis MOL361 (DSM-14220, DSMZ) was grown in Schaedler's Broth (BD Biosciences) in an anaerobic chamber of 5% hydrogen, 10% carbon dioxide and balanced nitrogen. *Bacteroides thetaiotaomicron* (ATCC 29148) was grown in Brain Heart Infusion media (BD Biosciences) supplemented with 5 ug/ml hemin (Frontier Scientific) and 0.5 ug/ml vitamin K1 (Sigma Aldrich) under the same anaerobic conditions. Mouse- and human-derived spore-forming bacterial consortia were isolated by chloroform treatment and propagated in mice as described in[3].

Heterologous expression in *B. theta*

CUW_0748 from *T. sanguinis* MOL361was PCR amplified and cloned into the expression vector pFD340 using one-step sequence- and ligation-independent cloning (SLIC) protocols described in [49]. The vector was transformed into *E. coli* with selection using 100 ug/ml ampicillin and conjugated into *B. theta* using the *E. coli* helper plasmid RK231 with 50 ug/ml kanamycin selection. *E. coli* was killed using 200 ug/ml gentamicin and transconjugant strains were selected using 5 ug/ml erythromycin. Successful conjugation and gene expression were confirmed by PCR and qPCR for CUW_0748 in DNA and RNA extracted from *B. theta* clones.

Turicibacter colonization of germ-free mice

T. sanguinis MOL361 was anaerobically cultured as described above, washed, pelleted and re- suspended at 106 cfu/ml in pre-reduced PBS. GF mice were gavaged with 200 ul bacterial suspension and maintained under sterile conditions for at least 2 weeks.

APP+ uptake assay

T. sanguinis and *B. theta* were cultured anaerobically as described above and subcultured for 15– 17 hours to reach stationary phase. Bacterial APP+ transport activity was measured according to the manufacturer's instructions using the Neurotransmitter Transporter Uptake Assay Kit (Molecular Devices). Briefly, cells were pre-treated with vehicle, 20 nM to 200 uM unlabeled 5- HT (Sigma Aldrich), fluoxetine (Tocris), dopamine (Sigma Aldrich) or norepinephrine (Sigma Aldrich) for 30 min at 37°C. Dosages were determined based on physiologically- and pharmacologically-relevant concentrations of ~170 uM 5-HT in mouse colon[3] and ~130 uM fluoxetine scaled from human clinical treatments[50], respectively. Then cells were treated with APP+ for 4 hours at 37°C. Intracellular fluorescence signal was measured at 520 nm using a multimodal plate reader (Biotek Synergy H1). Bacterial suspensions were mounted on slides and imaged using an epifluorescence microscope (EVOS). Images of *B. theta* were brightened by 90% to resolve fluorescence signal.

[3H]5-HT, [3H]NE and [3H]Trp uptake assays—*T. sanguinis* or *B. theta* was cultured anaerobically as described above and subcultured for 15–17 hours to reach stationary phase. Cells were washed and resuspended in Kreb-Ringer's buffer, then left untreated or pre-treated with vehicle, unlabeled 5-HT (Sigma Aldrich), fluoxetine (Santa Cruz), reserpine (Sigma Aldrich) or tetrabenazine (Sigma Aldrich) for 30 min at 37°C. Cells were then incubated with 1 uM tritiated 5-HT (plus 0–500 uM unlabeled 5-HT for dose-dependent

assays), NE or Trp (Perkin Elmer). For *T. sanguinis*, all uptake reactions were performed at room temperature. For *B. theta*, uptake reactions were performed at either room temperature or 37°C.

Uptake reactions were terminated by washing in ice cold Kreb-Ringer's buffer. Washed *T. sanguinis* was trapped through 0.45 um PVDF filters on MultiScreenHTS plates connected to a vacuum manifold (EMD Millipore). For *B. theta*, washed cells were either trapped through 0.45 um PVDF filters or lysed by incubating in TE buffer plus triton and lysozyme. Extracted filters or lysed cells were incubated in 4 ml Filter Count scintillation fluid (Perkin Elmer) for 1 hour at room temp and radioactivity was measured using a liquid scintillation counter (Beckman LS6500).

Bacterial transcriptomic analysis

T. sanguinis was cultured anaerobically as described above and subcultured to mid-log-phase. Cells were incubated in culture media supplemented with vehicle, 200 uM 5-HT (Sigma Aldrich), fluoxetine (Tocris) or 5-HT with fluoxetine for 4 hours at 37°C. Bacteria were washed with PBS and lysed in TE buffer containing 1.2% Triton X100 and 15 mg/ml lysozyme. RNA was extracted using the RNAeasy Mini kit with on-column genomic DNA-digest (Qiagen). cDNA synthesis was performed using the qScript cDNA synthesis kit (Quantabio). RNA quality of RIN > 8.0 was confirmed using the 4200 Tapestation system (Agilent). rRNA were removed with the Ribo-Zero Bacterial kit (Illumina), RNA was prepared using the TruSeq Stranded RNA kit (Illumina) and 2 × 75 bp paired end reads were sequenced using the Illumina HiSeq platform by the UCLA Neuroscience Genomics Core. The bacterial RNAseq analysis package Rockhopper[51] was used for quality filtering, mapping against the *T. sanguinis* PC909 genome and differential expression analysis. Over 23.79 million reads were obtained for each sample, with 86–88% aligning to protein- coding genes. Heatmaps containing differentially expressed genes with adjusted $p < 0.05$ and coefficient of variation (standard deviation / mean) < 3 were generated using the pheatmap package for R. GO term enrichment analysis of differentially expressed genes with adjusted $p < 0.05$ was conducted using DAVID[52]. Functional protein networks were generated with differentially expressed genes with adjusted $p < 0.05$ using STRING[53].

Bacterial FM 4–64 staining and imaging

Overnight cultures of *T. sanguinis* MOL361 were pooled and treated with vehicle, 5-HT (200 uM), fluoxetine (200 uM) or 5-HT and fluoxetine (both 200 uM) for 24 hours at 37°C. Cells were washed with PBS, fixed in 4% PFA, and stained with FM4–64 (5 ug/ml) and DAPI (0.2 ug/ml) according to manufacturer's instructions. Cells were wet-mounted on glass slides and cover slips. Images were acquired at 63X using the Zeiss LSM 780 confocal microscope. Images were analyzed using Fiji software[54] by a researcher blinded to experimental group. FM 4–64 puncta were counted manually based on circularity and fluorescence intensity. Counts were normalized to cell area as determined by thresholding of DAPI staining.

Turicibacter colonization of antibiotic-treated mice

SPF mice were treated with ampicillin, gentamicin, neomycin and vancomycin (AGNV) in their drinking water at 0.5 g/L for 4 days. Fecal samples were collected and plated anaerobically to confirm bacterial clearance. After an additional day on sterile water, antibiotic-treated mice were orally gavaged once daily for 5 days with 106 cfu/mouse *T. sanguinis* MOL361 that was pre-treated with 200 uM 5-HT, fluoxetine or vehicle for 4 hours at 37°C. Mice were also maintained on regular water, 5-HT (24 μg/ml) or 5-HT (24 μg/ml) with fluoxetine (40 μg/ml) in the drinking water over the same 5 days of *Turicibacter* oral gavage. Fluoxetine drinking water concentration was determined so each mouse would receive an effective dose of 10 mg/kg/day. 5-HT drinking water concentration was determined by calculating the same molar concentration as Flx in drinking water. This dose of 5-HT elevated fecal levels by approximately 6-fold over vehicle. Three days after the final gavage, mice were euthanized by CO2 and the small and large intestines were collected for FISH as described below and lumenal contents from the small and large intestines were harvested for 16S rDNA sequencing. In the “drinking water only” experimental approach, mice were gavaged with untreated *T. sanguinis* once daily for 5 days and maintained on regular water, 5-HT or 5-HT with fluoxetine in the drinking water. Tissues were collected and analyzed 3 days after the final gavage. In the “bacterial pre-treatment only” experimental approach, mice were gavaged with one or three doses of vehicle, 5-HT, or 5-HT with fluoxetine-pretreated *T. sanguinis* once daily and sacrificed 12–24 hours after the final gavage.

Bacterial Fluorescence *In Situ* Hybridization (FISH)

Mouse intestines were fixed in Carnoys fixative overnight at 4°C, washed and transferred to 70% ethanol. Intestinal samples were then paraffin-embedded and cut into 5 μm longitudinal sections by IDEXX Bioresearch. Slides were deparaffinized with xylene, rehydrated in ethanol and incubated in 1 μM FISH probe (Sigma Aldrich) in hybridization buffer (0.9 M NaCl, 20 mM Tris HCl, pH 7.2, 0.1% SDS) for 4 hours at 50°C in a humidified chamber. *Turicibacter* probe TUR176 was used: 5’ [6FAM]-GCAYCTTTAAACTTTCGTCCTATCCG. Slides were then washed 3 times in pre-heated wash buffer (0.9 M NaCl, 20 mM Tris-HCl, pH 7.2) and mounted with ProLong Gold Antifade Mountant with DAPI (Invitrogen). Images were acquired on a Zeiss LSM 780 confocal microscope at 20X magnification. Image analyses were performed using ImageJ.

Fluoxetine treatment for 16S rDNA sequencing

SPF mice were orally gavaged daily for 7 days with 10 mg/kg fluoxetine (Santa Cruz) or treated with fluoxetine (40 μg/ml) in the drinking water for 14 days as indicated in figure legends. Fecal samples were harvested on day 0, 1, 4, 7 or 14 of treatment as indicated in figure legends and processed for 16S rDNA sequencing as described above.

Intestinal transcriptomic analysis

1 cm sections of the terminal ileum and distal colon were harvested from SPF, GF or *Turicibacter* monocolonized mice, washed with PBS to remove lumenal contents and homogenized using 5 mm stainless steel beads (Qiagen) for 1 min in a Mini-Beadbeater-16

(Biospec Products). RNA was extracted using the RNAeasy Mini kit with on-column genomic DNA-digest (Qiagen), and cDNA synthesis was performed using the qScript cDNA synthesis kit (Quantabio). RNA quality of RIN> 8.9 was confirmed using the 4200 Tapestation system (Agilent). RNA was prepared using the QuantSeq mRNA-Seq Library Prep kit (Lexogen) and 1 × 65 bp 3' reads were sequenced using the Illumina HiSeq platform by the UCLA Neuroscience Genomics Core. The Bluebee analysis platform (Lexogen) was used for quality filtering and mapping. Differential expression analysis was conducted using DESeq2[55]. At least 8.47 million aligned reads were obtained for each sample. Heatmaps containing differentially expressed genes with $q < 0.05$ were generated using the pheatmap package for R. GO term enrichment analysis of differentially expressed genes with $q < 0.05$ was conducted using DAVID[52].

Lipid clinical chemistry analysis

Serum samples were collected from SPF, GF, *Turicibacter*-monocolonized or *Turicibacter*-enriched mice and submitted to Charles River Clinical Pathology for analysis of lipid species including total cholesterol, free fatty acids, high-density lipoprotein, low-density lipoprotein and total triglycerides.

Serum lipidomic analysis

Lipids from 25 ul of plasma were extracted using a modified Bligh and Dyer extraction method by the UCLA lipidomics core facility[56]. Prior to biphasic extraction, a 13-lipid class Lipidyzer Internal Standard Mix is added to each sample (AB Sciex, 5040156). Following two successive extractions, pooled organic layers were dried down in a Genevac EZ-2 Elite evaporator. Lipid samples were resuspended in 1:1 methanol/dichloromethane with 10mM ammonium acetate and transferred to robovials (Thermo 10800107) for analysis. Samples were analyzed on the Sciex Lipidyzer Platform for targeted quantitative measurement of 1100 lipid species across 13 classes. Differential Mobility Device on Lipidyzer was tuned with SelexION tuning kit (Sciex 5040141). Instrument settings, tuning settings, and MRM list are available upon request.

Adipocyte histology and imaging

Epididymal, gonadal and inguinal white adipose tissues were collected from SPF, GF and *Turicibacter*-monocolonized mice. Tissues were weighed, fixed in 4% PFA for 48 hours, transferred to 70% ethanol, and submitted to IDEXX Pathology Services for paraffin sectioning and embedding. 5 um sections were stained with H&E and imaged at 20X magnification.

Adipocyte cell morphology and number were quantified using ImageJ.

Statistical Methods

All statistical data are included in Supplementary Table 11. Statistical analysis was performed using Prism software (GraphPad). Data were plotted in the figures as mean ± SEM. For each figure, n = the number of independent biological replicates. Differences between two treatment groups were assessed using two-tailed, unpaired Student t test with Welch's correction. Differences among > 2 groups with only one variable were assessed

using one-way ANOVA with Bonferroni post hoc test. Taxonomic comparisons from 16S rDNA sequencing analysis were analyzed by Kruskal-Wallis test with Bonferroni post hoc test. Two-way ANOVA with Bonferroni post-hoc test was used for ≥ 2 groups with two variables. Significant differences emerging from the above tests are indicated in the figures by *$p < 0.05$, **$p < 0.01$, ***$p < 0.001$, ****$p < 0.0001$ Notable near-significant differences ($0.5 < p < 0.1$) are indicated in the figures. Notable non-significant (and non-near significant) differences are indicated in the figures by “n.s.”.

Data Availability

Data generated or analyzed during this study are included in this published article and its supplementary information files. Structural modeling files that support the findings of this study are available from Zenodo with the identifier doi: 10.5281/zenodo.3266444. The 16S rDNA sequencing data that support the findings of this study are available from the Qiita database with study IDs 12585, 12596, and 12597 and are also available in the Supplementary Tables.

Bacterial transcriptomic data that support the findings of this study are available in Gene Expression Omnibus (GEO) repository with the accession number GSE133810 and are also available in the Supplementary Tables. Intestinal transcriptomic data that support the findings of this study are available in GEO repository with the accession number GSE133809 and are also available in the Supplementary Tables.

Supplementary Material

Refer to Web version on PubMed Central for supplementary material.

Acknowledgments

We thank members of the Hsiao lab and Gregory Donaldson for critical review of the manuscript; Ron Kaback (UCLA), Dongxue Yang and Eric Gouaux (Vollum Institute, OHSU), KC Huang (Stanford), Matthias Quick and Jonathan Javitch (Columbia University) for helpful advice; John Murowski, David Nusbaum and Jessica Yano (UCLA) for assistance with initial pilot experiments; Yanling Wang and Jeffrey F. Miller (UCLA) for providing *Bacteroides* strains and expression constructs; Kevin Williams (UCLA lipidomic core facility) for performing lipidomic measurements; Peter Bradley and Robert Gunsalus (UCLA) for facilitating radioisotope experiments; Gerard Karsenty (Columbia), Yin Tintut (UCLA), and Fredrik Bäckhed (University of Gothernburg) for providing *Tph1* mice and mouse samples. Support for this research was provided by the NIH Director’s Early Independence Award (5DP5OD017924) to E.Y.H., Klingenstein-Simons Award to E.Y.H., Packard Fellowship in Science and Engineering to E.Y.H., UPLIFT: UCLA Postdocs’ Longitudinal Investment in Faculty (Award # K12 GM106996) to H.E.V., Ruth L. Kirschstein National Research Service (Award # AI007323) to G.N.P. and the Division of Intramural Research of the NIH, National Institute of Neurological Disorders and Stroke to L.R.F. All data and materials to understand and assess the conclusions of this research are available in the main text and supplementary materials.

References

1. Vuong HE, Yano JM, Fung TC & Hsiao EY The Microbiome and Host Behavior. Annu Rev Neurosci 40, 21–49, doi:10.1146/annurev-neuro-072116-031347 (2017). [PubMed: 28301775]
2. Gershon MD & Tack J The serotonin signaling system: from basic understanding to drug development for functional GI disorders. Gastroenterology 132, 397–414, doi:10.1053/j.gastro.2006.11.002 (2007). [PubMed: 17241888]

3. Reigstad CS et al. Gut microbes promote colonic serotonin production through an effect of short-chain fatty acids on enterochromaffin cells. FASEB J 29, 1395–1403, doi:10.1096/fj.14-259598 (2015). [PubMed: 25550456]
4. Wikoff WR et al. Metabolomics analysis reveals large effects of gut microflora on mammalian blood metabolites. PloS one 106, 3698–3703, doi:10.1371/journal.pone.018074510.1073/pnas.0812874106 (2009).
5. Yano JM et al. Indigenous bacteria from the gut microbiota regulate host serotonin biosynthesis. Cell 161, 264–276, doi:10.1016/j.cell.2015.02.047 (2015). [PubMed: 25860609]
6. Sjogren K et al. The gut microbiota regulates bone mass in mice. J Bone Miner Res 27, 1357–1367, doi:10.1002/jbmr.1588 (2012). [PubMed: 22407806]
7. Hata T et al. Regulation of gut luminal serotonin by commensal microbiota in mice. PloS one 12, e0180745, doi:10.1371/journal.pone.0180745 (2017). [PubMed: 28683093]
8. Fujimiya M, Okumiya K & Kuwahara A Immunoelectron microscopic study of the luminal release of serotonin from rat enterochromaffin cells induced by high intraluminal pressure. Histochem Cell Biol 108, 105–113 (1997). [PubMed: 9272429]
9. Mawe GM & Hoffman JM Serotonin signalling in the gut--functions, dysfunctions and therapeutic targets. Nat Rev Gastroenterol Hepatol 10, 473–486, doi:10.1038/nrgastro.2013.105 (2013). [PubMed: 23797870]
10. Chen JJ et al. Maintenance of serotonin in the intestinal mucosa and ganglia of mice that lack the high-affinity serotonin transporter: Abnormal intestinal motility and the expression of cation transporters. The Journal of neuroscience : the official journal of the Society for Neuroscience 21, 6348–6361 (2001). [PubMed: 11487658]
11. Olivella M, Gonzalez A, Pardo L & Deupi X Relation between sequence and structure in membrane proteins. Bioinformatics 29, 1589–1592, doi:10.1093/bioinformatics/btt249 (2013). [PubMed: 23677941]
12. Coleman JA & Gouaux E Structural basis for recognition of diverse antidepressants by the human serotonin transporter. Nat Struct Mol Biol 25, 170–175, doi:10.1038/s41594-018-0026-8 (2018). [PubMed: 29379174]
13. Forrest LR, Tavoulari S, Zhang YW, Rudnick G & Honig B Identification of a chloride ion binding site in Na+/Cl -dependent transporters. Proceedings of the National Academy of Sciences of the United States of America 104, 12761–12766, doi:10.1073/pnas.0705600104 (2007). [PubMed: 17652169]
14. Barker EL, Moore KR, Rakhshan F & Blakely RD Transmembrane domain I contributes to the permeation pathway for serotonin and ions in the serotonin transporter. J Neurosci 19, 4705–4717 (1999). [PubMed: 10366604]
15. Solis E Jr. et al. 4-(4-(dimethylamino)phenyl)-1-methylpyridinium (APP+) is a fluorescent substrate for the human serotonin transporter. J Biol Chem 287, 8852–8863, doi:10.1074/jbc.M111.267757 (2012). [PubMed: 22291010]
16. Chanrion B et al. Physical interaction between the serotonin transporter and neuronal nitric oxide synthase underlies reciprocal modulation of their activity. Proceedings of the National Academy of Sciences of the United States of America 104, 8119–8124, doi:10.1073/pnas.0610964104 (2007). [PubMed: 17452640]
17. Seimandi M et al. Calcineurin interacts with the serotonin transporter C-terminus to modulate its plasma membrane expression and serotonin uptake. J Neurosci 33, 16189–16199, doi:10.1523/JNEUROSCI.0076-13.2013 (2013). [PubMed: 24107951]
18. Ramijan K et al. Stress-induced formation of cell wall-deficient cells in filamentous actinomycetes. Nat Commun 9, 5164, doi:10.1038/s41467-018-07560-9 (2018). [PubMed: 30514921]
19. Browne HP et al. Culturing of 'unculturable' human microbiota reveals novel taxa and extensive sporulation. Nature 533, 543–546, doi:10.1038/nature17645 (2016). [PubMed: 27144353]
20. Goodrich JK, Davenport ER, Waters JL, Clark AG & Ley RE Cross-species comparisons of host genetic associations with the microbiome. Science 352, 532–535, doi:10.1126/science.aad9379 (2016). [PubMed: 27126034]
21. Geva-Zatorsky N et al. Mining the Human Gut Microbiota for Immunomodulatory Organisms. Cell 168, 928–943 e911, doi:10.1016/j.cell.2017.01.022 (2017). [PubMed: 28215708]

22. Miyazaki M, Dobrzyn A, Elias PM & Ntambi JM Stearoyl-CoA desaturase-2 gene expression is required for lipid synthesis during early skin and liver development. Proceedings of the National Academy of Sciences of the United States of America 102, 12501–12506, doi:10.1073/pnas.0503132102 (2005). [PubMed: 16118274]
23. Porter NT, Canales P, Peterson DA & Martens EC A Subset of Polysaccharide Capsules in the Human Symbiont Bacteroides thetaiotaomicron Promote Increased Competitive Fitness in the Mouse Gut. Cell host & microbe 22, 494–506 e498, doi:10.1016/j.chom.2017.08.020 (2017). [PubMed: 28966055]
24. Lyte M, Villageliu DN, Crooker BA & Brown DR Symposium review: Microbial endocrinology-Why the integration of microbes, epithelial cells, and neurochemical signals in the digestive tract matters to ruminant health. J Dairy Sci 101, 5619–5628, doi:10.3168/jds.2017-13589 (2018). [PubMed: 29550113]
25. Jackson MA et al. Gut microbiota associations with common diseases and prescription medications in a population-based cohort. Nat Commun 9, 2655, doi:10.1038/s41467-018-05184-7 (2018). [PubMed: 29985401]
26. Goodrich JK et al. Genetic Determinants of the Gut Microbiome in UK Twins. Cell Host Microbe 19, 731–743, doi:10.1016/j.chom.2016.04.017 (2016). [PubMed: 27173935]
27. Bernstein CN & Forbes JD Gut Microbiome in Inflammatory Bowel Disease and Other Chronic Immune-Mediated Inflammatory Diseases. Inflamm Intest Dis 2, 116–123, doi:10.1159/000481401 (2017). [PubMed: 30018962]
28. Guo X et al. High Fat Diet Alters Gut Microbiota and the Expression of Paneth Cell- Antimicrobial Peptides Preceding Changes of Circulating Inflammatory Cytokines. Mediators Inflamm 2017, 9474896, doi:10.1155/2017/9474896 (2017). [PubMed: 28316379]
29. Lee SH, Paz-Filho G, Mastronardi C, Licinio J & Wong ML Is increased antidepressant exposure a contributory factor to the obesity pandemic? Transl Psychiatry 6, e759, doi:10.1038/tp.2016.25 (2016). [PubMed: 26978741]
30. Beyazyuz M, Albayrak Y, Egilmez OB, Albayrak N & Beyazyuz E Relationship between SSRIs and Metabolic Syndrome Abnormalities in Patients with Generalized Anxiety Disorder: A Prospective Study. Psychiatry Investig 10, 148–154, doi:10.4306/pi.2013.10.2.148 (2013).

Methods References

31. Abdala-Valencia H et al. Inhibition of allergic inflammation by supplementation with 5-hydroxytryptophan. Am J Physiol Lung Cell Mol Physiol 303, L642–660, doi:10.1152/ajplung.00406.2011 (2012). [PubMed: 22842218]
32. Caporaso JG et al. Global patterns of 16S rRNA diversity at a depth of millions of sequences per sample. Proceedings of the National Academy of Sciences of the United States of America 108 Suppl 1, 4516–4522, doi:10.1073/pnas.1000080107 (2011). [PubMed: 20534432]
33. Caporaso JG et al. QIIME allows analysis of high-throughput community sequencing data. Nature methods 7, 335–336, doi:10.1038/nmeth.f.303 (2010). [PubMed: 20383131]
34. Langille MG et al. Predictive functional profiling of microbial communities using 16S rRNA marker gene sequences. Nat Biotechnol 31, 814–821, doi:10.1038/nbt.2676 (2013). [PubMed: 23975157]
35. Katoh K, Rozewicki J & Yamada KD MAFFT online service: multiple sequence alignment, interactive sequence choice and visualization. Brief Bioinform, doi:10.1093/bib/bbx108 (2017).
36. Robinson O, Dylus D & Dessimoz C Phylo.io: Interactive Viewing and Comparison of Large Phylogenetic Trees on the Web. Mol Biol Evol 33, 2163–2166, doi:10.1093/molbev/msw080 (2016). [PubMed: 27189561]
37. Kelley LA, Mezulis S, Yates CM, Wass MN & Sternberg MJ The Phyre2 web portal for protein modeling, prediction and analysis. Nat Protoc 10, 845–858, doi:10.1038/nprot.2015.053 (2015). [PubMed: 25950237]
38. Webb B & Sali A Comparative Protein Structure Modeling Using MODELLER. Curr Protoc Protein Sci 86, 2 9 1–2 9 37, doi:10.1002/cpps.20 (2016).

39. Berman HM et al. The Protein Data Bank. Nucleic Acids Res 28, 235–242 (2000). [PubMed: 10592235]
40. Stamm M, Staritzbichler R, Khafizov K & Forrest LR AlignMe--a membrane protein sequence alignment web server. Nucleic Acids Res 42, W246–251, doi:10.1093/nar/gku291 (2014). [PubMed: 24753425]
41. Wallner B ProQM-resample: improved model quality assessment for membrane proteins by limited conformational sampling. Bioinformatics 30, 2221–2223, doi:10.1093/bioinformatics/btu187 (2014). [PubMed: 24713439]
42. Laskowski RA, Rullmannn JA, MacArthur MW, Kaptein R & Thornton JM AQUA and PROCHECK-NMR: programs for checking the quality of protein structures solved by NMR. J Biomol NMR 8, 477–486 (1996). [PubMed: 9008363]
43. Best RB et al. Optimization of the additive CHARMM all-atom protein force field targeting improved sampling of the backbone phi, psi and side-chain chi(1) and chi(2) dihedral angles. J Chem Theory Comput 8, 3257–3273, doi:10.1021/ct300400x (2012). [PubMed: 23341755]
44. Phillips JC et al. Scalable molecular dynamics with NAMD. J Comput Chem 26, 1781–1802, doi: 10.1002/jcc.20289 (2005). [PubMed: 16222654]
45. Williams CJ et al. MolProbity: More and better reference data for improved all-atom structure validation. Protein Sci 27, 293–315, doi:10.1002/pro.3330 (2018). [PubMed: 29067766]
46. Ashkenazy H et al. ConSurf 2016: an improved methodology to estimate and visualize evolutionary conservation in macromolecules. Nucleic Acids Res 44, W344–350, doi:10.1093/nar/gkw408 (2016). [PubMed: 27166375]
47. Pettersen EF et al. UCSF Chimera--a visualization system for exploratory research and analysis. J Comput Chem 25, 1605–1612, doi:10.1002/jcc.20084 (2004). [PubMed: 15264254]
48. Coleman JA, Green EM & Gouaux E X-ray structures and mechanism of the human serotonin transporter. Nature 532, 334–339, doi:10.1038/nature17629 (2016). [PubMed: 27049939]
49. Forrest LR, Tavoulari S, Zhang YW, Rudnick G & Honig B Identification of a chloride ion binding site in Na+/Cl -dependent transporters. Proceedings of the National Academy of Sciences of the United States of America 104, 12761–12766, doi:10.1073/pnas.0705600104 (2007). [PubMed: 17652169]
50. Barker EL, Moore KR, Rakhshan F & Blakely RD Transmembrane domain I contributes to the permeation pathway for serotonin and ions in the serotonin transporter. J Neurosci 19, 4705–4717 (1999). [PubMed: 10366604]
51. Yano JM et al. Indigenous bacteria from the gut microbiota regulate host serotonin biosynthesis. Cell 161, 264–276, doi:10.1016/j.cell.2015.02.047 (2015). [PubMed: 25860609]
52. Jeong JY et al. One-step sequence- and ligation-independent cloning as a rapid and versatile cloning method for functional genomics studies. Appl Environ Microbiol 78, 5440–5443, doi: 10.1128/AEM.00844-12 (2012). [PubMed: 22610439]
53. Hiemke C & Hartter S Pharmacokinetics of selective serotonin reuptake inhibitors. Pharmacol Ther 85, 11–28 (2000). [PubMed: 10674711]
54. McClure R et al. Computational analysis of bacterial RNA-Seq data. Nucleic Acids Res 41, e140, doi:10.1093/nar/gkt444 (2013). [PubMed: 23716638]
55. Huang da W, Sherman BT & Lempicki RA Systematic and integrative analysis of large gene lists using DAVID bioinformatics resources. Nat Protoc 4, 44–57, doi:10.1038/nprot.2008.211 (2009). [PubMed: 19131956]
56. Szklarczyk D et al. The STRING database in 2017: quality-controlled protein-protein association networks, made broadly accessible. Nucleic Acids Res 45, D362–D368, doi:10.1093/nar/gkw937 (2017). [PubMed: 27924014]
57. Schindelin J et al. Fiji: an open-source platform for biological-image analysis. Nat Methods 9, 676–682, doi:10.1038/nmeth.2019 (2012). [PubMed: 22743772]
58. Love MI, Huber W & Anders S Moderated estimation of fold change and dispersion for RNA-seq data with DESeq2. Genome biology 15, 550, doi:10.1186/s13059-014-0550-8 (2014). [PubMed: 25516281]
59. Bligh EG & Dyer WJ A rapid method of total lipid extraction and purification. Can J Biochem Physiol 37, 911–917, doi:10.1139/o59-099 (1959). [PubMed: 13671378]

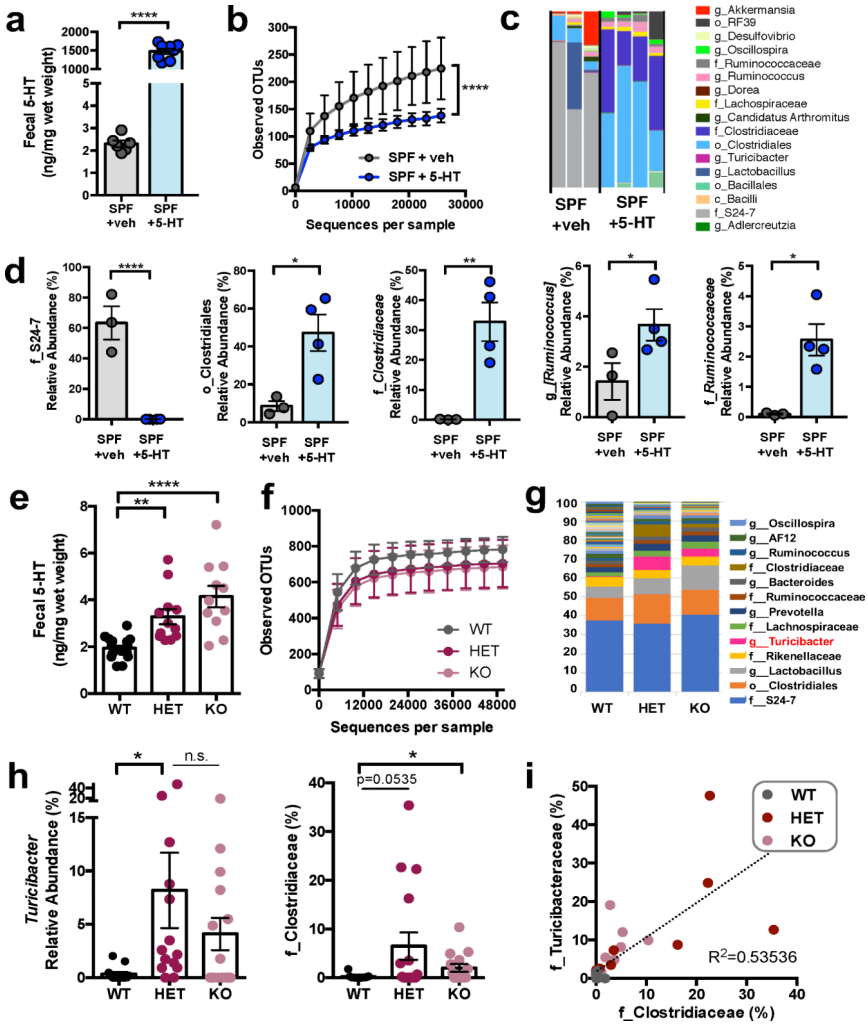

Figure 1: Elevating intestinal 5-HT enriches for spore-forming bacteria in the gut.

a, Fecal 5-HT levels from SPF mice orally supplemented with 5-HT or vehicle in drinking water (two- tailed, unpaired Student's t-test; n = 6, 8 cages). **b**, Alpha-diversity of OTUs derived from 16S rDNA sequencing of feces following vehicle vs. 5-HT treatment (two-way ANOVA with Bonferroni, n=3, 4 cages). **c**, Taxonomic diversity of the fecal microbiota after vehicle vs. 5-HT treatment (n=3, 4 cages). **d**, Relative abundance of bacterial taxa in fecal microbiota after vehicle vs. 5-HT treatment (two-way ANOVA with Kruskal-Wallis, n=3, 4 cages). **e**, Fecal 5-HT levels from SPF wild-type (WT), $SERT^{+/-}$ (HET) and $SERT^{-/-}$ (KO) mice. (one-way ANOVA with Bonferroni, n=13–15 cages). **f**, Alpha-diversity of OTUs derived from 16S rDNA sequencing of feces from SERT-deficient mice relative to WT controls (n=10–12 cages). **g**, Taxonomic diversity of the fecal microbiota after vehicle vs. 5-HT treatment (n=10–12 cages). **h**, Relative abundance of bacterial taxa in fecal microbiota of SERT-deficient mice relative to WT controls (one-way ANOVA with Kruskal Wallis, n=10, 11, 12 cages; n.s.: p=0.2134). **i**, Linear correlation between relative abundance of *Turicibacteraceae* vs. *Clostridiaceae* in fecal microbiota from SERT- deficient mice vs. WT controls (n=13, 15, 14 cages). (Mean ± SEM, * $p < 0.05$, ** $p < 0.01$, **** $p < 0.0001$, n.s.

= not statistically significant; refer to Supplementary Table 11 for detailed statistical information)

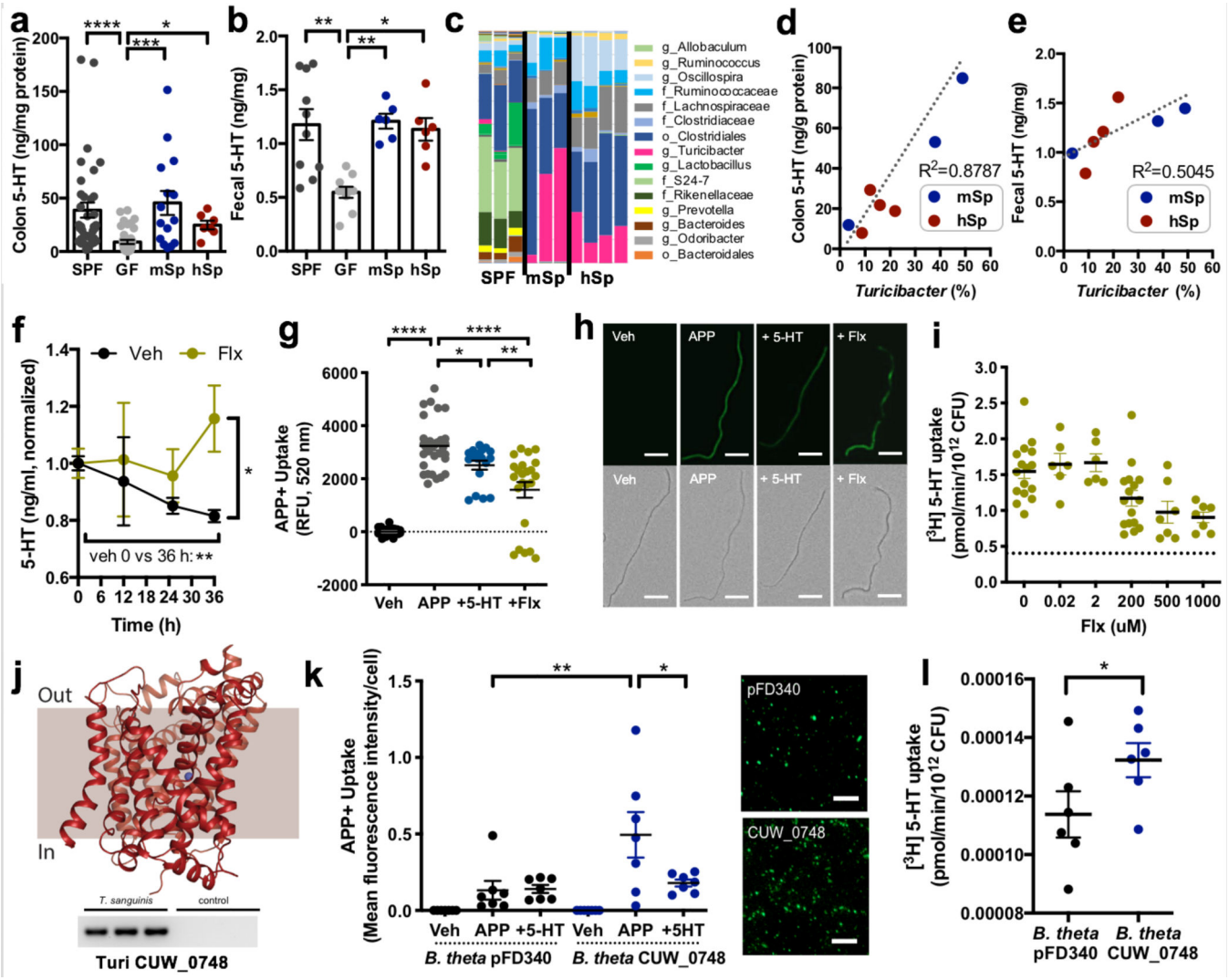

Figure 2: *Turicibacter sanguinis* uptakes 5-HT, which is inhibited by the selective serotonin reuptake inhibitor, fluoxetine.

a, Colon and fecal levels of 5-HT in mice that are conventionally colonized (SPF), germ-free (GF) or colonized with mouse-derived (m) or human-derived (h) spore-forming bacteria (Sp) (one-way ANOVA with Bonferroni, n=36, 37, 15, 7 mice). **b**, Fecal 5-HT in SPF, GF or mSp- or hSp-colonized mice (one-way ANOVA with Bonferroni, n=10, 10, 6, 6 mice). **c**, Taxonomic diversity of the fecal microbiota of SPF, mSp- and hSp-colonized mice (n=3, 4 cages). **d**, Linear correlation between fecal *Turicibacter* and colon 5-HT (n=3, 4 cages). **e**, Linear correlation between fecal *Turicibacter* and fecal 5-HT (n=3, 4 cages). **f**, 5-HT in supernatant after 0, 12, 25 and 36 hours of *T. sanguinis* MOL361 growth in Schaedler broth supplemented with vehicle or 200 uM fluoxetine (two-way ANOVA with Bonferroni, n=3, 4 cultures). **g**, Uptake by *T. sanguinis* exposed to vehicle (Veh) or APP+, either alone (APP) or with 200 uM 5-HT (+5-HT) or fluoxetine (+Flx) pre-treatment for 30 min (one-way ANOVA with Bonferroni, n=33, 33, 18, 23 cultures). **h**, Representative images of *T. sanguinis* exposed to Veh, APP, +5-HT or +Flx for 30 min (representing n=33, 33, 18, 23 cultures). Scale bar: 20 um. **i,** [3H] 5-HT uptake by *T. sanguinis* at 20 min after pre-

treatment with Veh or +Flx. Dotted line: average background signal in negative controls. (one-way ANOVA with Bonferroni, n=7–16 cultures). **j**, Top: Predicted structural model for the putative SERT ortholog CUW_0748 in *T. sanguinis* MOL361. Bottom: qPCR product for CUW_0748 cDNA generated from *T. sanguinis* RNA (n=3 cultures). **k**, APP+ uptake in *B. theta* expressing CUW_0748 or vector control (pFD340) at 20 min after exposure to Veh, APP or +5-HT (one-way ANOVA with Bonferroni, n=7 cultures). Right: Representative images of APP+ uptake in *B. theta* expressing CUW_0748 or pFD340 control, with brightness at 90% higher than that in panel H. Scale bar: 20 um. **l**, Uptake of 1 uM [3H] 5-HT by *B. theta* expressing CUW_0748 or pFD340 after 20 min (two-tailed unpaired Student's t-test, n=6 cultures). (Mean ± SEM, * $p < 0.05$, ** $p < 0.01$, *** $p < 0.001$, **** $p < 0.0001$, n.s. = not statistically significant; refer to Supplementary Table 11 for detailed statistical information)

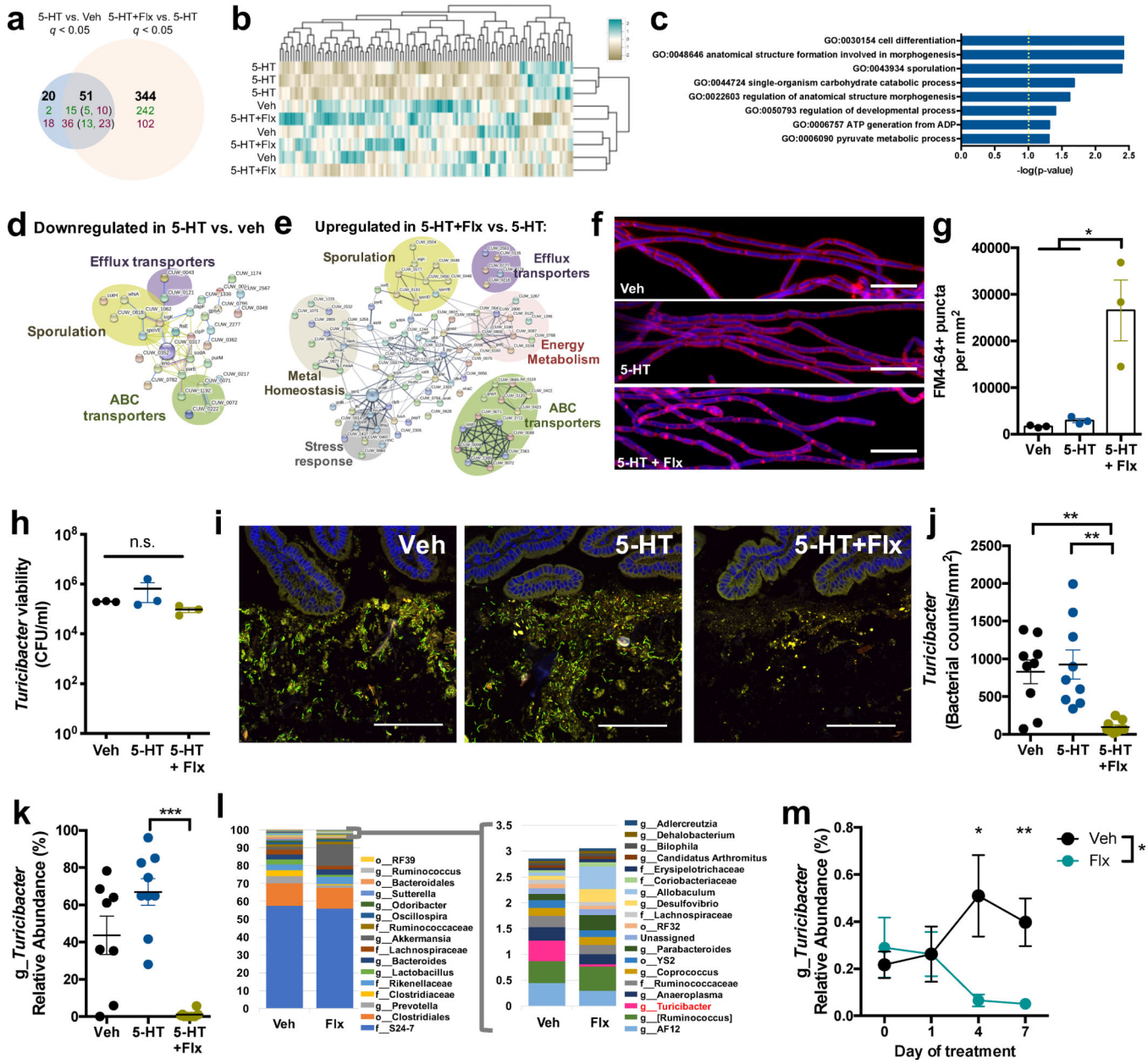

Figure 3: 5-HT and the selective serotonin reuptake inhibitor, fluoxetine, regulate gene expression and intestinal colonization of *Turicibacter sanguinis*.

a, Differentially expressed genes (q < 0.05) in *T. sanguinis* MOL361 after 4 hr exposure to vehicle, 200 uM 5-HT, or 5-HT with fluoxetine (Flx). Bold:total genes. Green:upregulated genes; red: downregulated genes. Numbers in parentheses: 5-HT-regulated genes that were further differentially expressed by Flx (Benjamini-Hochberg, n=3 cultures). **b**, Heatmap of genes with coefficient of variation < 3 (n=3 cultures). **c**, GO term enrichment analysis of genes differentially expressed in 5-HT vs. vehicle and 5-HT + Flx vs. 5-HT. (Fisher exact, n=3 cultures) **d**, Protein network analysis of 54 genes downregulated in *T. sanguinis* treated with 5-HT vs. vehicle. (n=3 cultures) **e**, Protein network analysis of 257 genes upregulated in *T. sanguinis* treated with 5-HT + Flx vs. 5-HT. (n=3 cultures) **f**, Representative images of

T. sanguinis treated for 4 hr with vehicle, 200 uM 5-HT, or 5-HT with Flx, and stained with FM 4–64 membrane dye (pink) and DAPI (blue). (n=3 cultures). Scale bar: 10 um. **g**, Number of FM 4–64 puncta per area of *T. sanguinis* (one-way ANOVA with Bonferroni, n=3 cultures). **h**, Viability of *T. sanguinis* after 4 hr exposure to vehicle, 200 uM 5- HT, or 5-HT with Flx. (one-way ANOVA with Bonferroni, n=3 cultures; n.s.: p=0.9891). **i**, Representative FISH images of *T. sanguinis* (green) and small intestinal epithelial cells (DAPI, blue) from antibiotic-treated mice at 3 days after gavage with *T. sanguinis* pre-treated for 4 hr with vehicle, 200 uM 5-HT, or 5-HT with Flx (n=9 cages). Scale bar: 100 um. **j**, *T. sanguinis* cell counts from FISH images (one-way ANOVA with Bonferroni, n=9 cages). **k**, Relative abundance of *Turicibacter* by 16S rDNA sequencing of small intestinal lumenal contents (one- way ANOVA with Bonferroni, n=9 cages). **l**, Taxonomic diversity based on 16S rDNA sequencing of fecal microbiota on day 7 of Flx treatment. **m**, Relative abundance of *Turicibacter* in feces from SPF mice at 0, 1, 4, and 7 days after gavage with 10 mg/kg Flx (two-way ANOVA with Bonferroni, n=8, 18 cages). (Mean ± SEM, * $p < 0.05$, ** $p < 0.01$, *** $p < 0.001$, n.s. = not statistically significant; refer to Supplementary Table 11 for detailed statistical information).

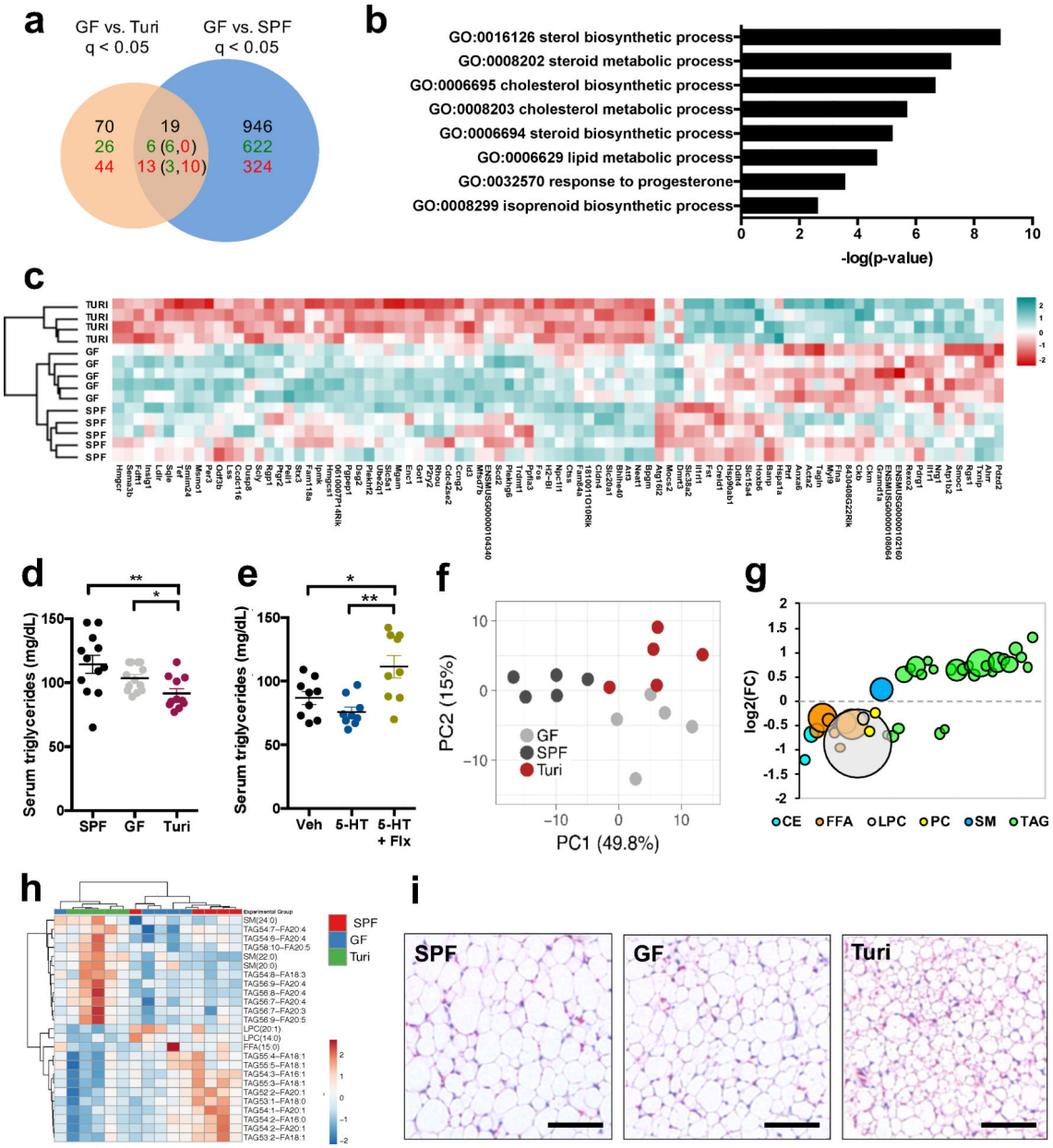

Figure 4: *Turicibacter sanguinis* colonization regulates host lipid metabolism.

a, Differentially expressed genes (q < 0.05) in small intestines from *T. sanguinis*-monocolonized, germ-free (GF) or SPF mice. Bolded numbers represent total differentially expressed genes. Numbers in green denote upregulated genes; numbers in red denote downregulated genes. Numbers in parentheses denote subsets of *T. sanguinis* regulated genes that were further differentially expressed by SPF (Wald test, n=5, 5, 4 mice). **b,** GO term enrichment analysis of genes differentially expressed in small intestine in response to *T. sanguinis* relative to GF controls (Fisher exact, n=4, 5, 5 mice). **c,** Heatmap of the 89 differentially expressed genes in the small intestine in response to *T. sanguinis* colonization (n=5, 5, 4 mice). **d,** Total serum triglyceride levels in GF, SPF and *T. sanguinis*-monocolonized mice (one-way ANOVA with Bonferroni, n=12, 13, 11 mice). **e,** Total serum

triglyceride levels from antibiotic-treated mice gavaged with *T. sanguinis* pre-treated for 4 hr with vehicle, 200 uM 5-HT, or 200 uM 5-HT with Flx (one-way ANOVA with Bonferroni, n=9 mice). **f,** Principal components analysis of serum lipidomic data for lipid species with $p < 0.05$ for *T. sanguinis* vs. GF and *T. sanguinis* vs. SPF mice (two-way ANOVA + Bonferroni, n=5 mice). **g,** Average fold change (FC) of serum lipid species ($p < 0.05$) differentially regulated by *T. sanguinis* compared to GF controls. Largest circle = $p < 0.001$, smallest circle = $p<0.05$. CE=cholesterol esters, FFA=free fatty acids, LPC=lysophosphatidylcholines, PC=phosphatidylcholines, SM=sphingomyelins, TAG=triacylglycerides. (two-way ANOVA + Bonferroni, n=5 mice). **h,** Heatmap of 25 serum lipid species similarly increased (red) or decreased (blue) by *T. sanguinis* colonization relative to both GF and SPF controls (n=5 mice). **i,** Representative image of inguinal white adipose tissue from GF, SPF and *T. sanguinis*-monocolonized mice. Scale bar = 100 um. (representing n=5 mice) (Mean ± SEM, * $p < 0.05$, ** $p < 0.01$, *** $p < 0.001$, **** $p < 0.0001$, n.s. = not statistically significant; refer to Supplementary Table 11 for detailed statistical information)